

Dynamic electrophoresis of concentrated droplet dispersions at arbitrary surface potentials

James Lou, Eric Lee*

Department of Chemical Engineering, Institute of Polymer Science and Engineering, National Taiwan University, Taipei, 10617 Taiwan

Received 30 January 2007; received in revised form 16 July 2007; accepted 16 July 2007

Available online 24 July 2007

Abstract

Dynamic electrophoresis of a dispersion of spherical droplets with arbitrary zeta potential and double layer thickness is analyzed in this study, based on Kuwabara's unit cell model. Pseudo-spectral method with Chebyshev polynomials is adopted to solve the corresponding general electrokinetic equations. Similar to the observations of hard spheres, the droplets exhibit non-linear phenomena such as maxima or minima on both mobility magnitude and phase lag with varying frequency of input alternative electric field, as the zeta potential of the droplets become high. Our results presented here add another dimension to the previous corresponding results of hard spheres, with the parameter of viscosity ratio, η_o/η_i , where η_o and η_i refer to the fluid viscosities outside and inside of the droplets, respectively. Consistent qualitative behaviors are observed with $\eta_o/\eta_i = 0$ representing the hard spheres situation. No abrupt change is observed associating with the phase change to the droplets. The dynamic mobility is found to be faster in magnitude, as might be expected.

© 2007 Elsevier Ltd. All rights reserved.

Keywords: Dynamic electrophoresis; Droplet; High zeta potential

1. Introduction

When an alternating voltage is applied to a colloid, the particles move back and forth at a velocity that depends on its size, zeta potential, and on the frequency of the applied field (Hunter, 1998; O'Brien et al., 1995; Mizuno et al., 2000; Dukhin et al., 2000). As they move, the particles generate sound waves, an effect generally referred to as the electrokinetic sonic amplitude, or ESA (O'Brien, 1988). Another related electroacoustic phenomenon is called vibration potential, or CVP, which states that a sound wave would generate an alternating electric field as it passes through a suspension of colloids. It turns out that CVP is the converse of ESA, while the latter has become dominant in the last two decades, due to the fact that apparently it is easier to measure the resulting sound waves than the tiny voltages, considering the electric noise associated with CVP (Hunter, 1998). ESA is able to provide reliable particle size information as well as zeta potential, especially for concentrated suspension of colloids. Compared with other techniques which usually

require dilution, the ESA can measure the concentrated sample in its natural state of interest. It has been found that dilution will significantly change the surface properties of the original suspension system (Hunter, 1998). This is the major advantage of the electroacoustic technique, such as ESA. A thorough review of the experimental development was provided by Hunter (1998). As for the theoretical part, O'Brien (1988) investigated the dynamic electrophoresis of a spherical rigid colloid with very thin double layer in a dilute dispersion. He derived a formula relating the measurable information of the output ESA signals to the dynamic electrophoretic mobility. The surface properties were obtainable once these data were established. Various attempts were made ever since to loosen the restriction encountered in O'Brien's work. For example, Mangelsdorf and White (1992) took into consideration the effect of double layer polarization and stern layer. Based on their studies, Ohshima (1996) derived an analytical expression for the case of low zeta potential. These studies were all focused on the dilute dispersion, i.e., a spherical particle in an infinite solution.

Later, Ohshima extended further to investigate the case of concentrated suspensions. According to his analysis, the dynamic electrophoretic mobility of the particle could be seriously

* Corresponding author. Tel./fax: +886 2 23622530.

E-mail address: ericlee@ntu.edu.tw (E. Lee).

influenced by the presence of neighboring particles (Ohshima, 1997, 1999a,b), indicating the complexity of concentrated dispersions.

Generally speaking, analytical approach is valid for the limiting cases of linearized electrokinetic equations. When non-linear effect is involved, for example, the complete non-linear Poisson–Boltzmann equation, it is impossible to solve it analytically under the conditions of arbitrary zeta potential and arbitrary double layer thickness. A numerical approach is necessary under the situation. As a result, the authors have conducted a series of numerical investigations in the field of electrokinetics, with polarization effect as the major factor of interest, which is generally not observable in traditional analytical approaches (Lee et al., 1999). For the dynamic electrophoresis in particular, several works (Lee et al., 2001, 2002a, 2003; Hsu et al., 2002; Lou et al., 2005) were reported by the authors regarding the rigid spheres. Typical non-linear phenomena due to polarization effect were generally observed, such as the exhibition of maxima or minima of mobility, as the frequency of the applied electric field was varied.

The electrophoresis of a dispersion of non-rigid entities has many applications in practice. Emulsion, sol, and foam, for instance, belong to this category. Compared with that of rigid entities, the analysis of non-rigid entities is more complicated because the electrokinetic equations for the space inside an entity and outside an entity need to be solved simultaneously. Several attempts have been made in the literature to model the static electrophoretic behavior of a dispersion of non-rigid entities. Booth (1951) first investigated the electrophoretic behavior of a mercury drop. Later on, Levine and O'Brien (1973) examined thoroughly the motion of a mercury drop and found that it can be influenced significantly by an externally applied static electric field. They found that the polarization effect is dominant in the electrophoresis of the mercury drop. Baygents and Saville (1991a,b) analyzed the electrophoretic mobility as a function of the zeta potential for conducting and non-conducting drops. Ohshima (1999c) also extended the study to concentrated dispersion of charged spherical mercury drops and derived a formula for it.

It should be noted that while there were many published reports on dynamic electrophoresis, essentially all were focused on the rigid particle. And while there are many studies on the electrophoresis of droplet dispersions, few if none of them are focused on the dynamic electrophoresis; essentially all of them are confined to the static electrophoresis. As a result, the authors studied the dynamic electrophoresis of a spherical droplet within a solid cavity (Lee et al., 2006). Indeed it is possible that the tiny electroacoustic vibration is able to penetrate the droplet interface and set the inner fluid into an internal flow, thus changing the overall dynamic behavior of the emulsions. It modeled the electrophoresis in a porous medium with special emphasis on the boundary effect. Polarization effect of double layer was found to be important. As for the dynamic electrophoresis of concentrated dispersion of droplets, the authors also presented a study confined to low zeta potential situation (Hsu et al., 2007). It was found there that the mobility is larger than the corresponding rigid particles as the frequency

gets higher. No polarization effect is involved, however, since the zeta potential is low.

As a conclusive generalization of the previous work, we consider here the dynamic electrophoresis of spherical droplets with arbitrary zeta potential and double layer thickness, as well as arbitrary volume fraction of droplets. The double layer and polarization overlapping effect are taken into account. Kuwabara's (1959) unit cell model is adopted with the boundary conditions on cell surface proposed by Shilov et al. (1981), which has been found to give better experimental agreement in many other related works on electrokinetic phenomena, as concentrated suspension is considered. A pseudo-spectral method based on Chebyshev polynomials is adopted to solve the resultant governing equations subject to the associated boundary conditions. The method has proved to be both powerful and accurate in solving the general electrokinetic equations, static or dynamic (Lee et al., 1999, 2001). Moreover, it also prevailed in the analyses of polymeric fluid flow, as published by the authors (Lee et al., 2002b, 2004). Various important factors are examined, such as the frequency of the applied electric field, the volume fraction of droplets, the thickness of the double layer, and the relative viscosity of the droplet fluid. Its influences on the dynamic electrophoretic behavior of the dispersion are thoroughly explored and discussed in this study.

2. Theory

Consider the electrophoretic problem illustrated in Fig. 1 where a dispersion of electrolyte-free drops of radius a move with a velocity $\mathbf{U} = Ue^{-i\omega t}\mathbf{e}_z$ under an applied electric field $\mathbf{E} = E_z e^{-i\omega t}\mathbf{e}_z$ back and forth in the z -direction. Note that both \mathbf{U} and \mathbf{E} are complex quantities with real and imaginary

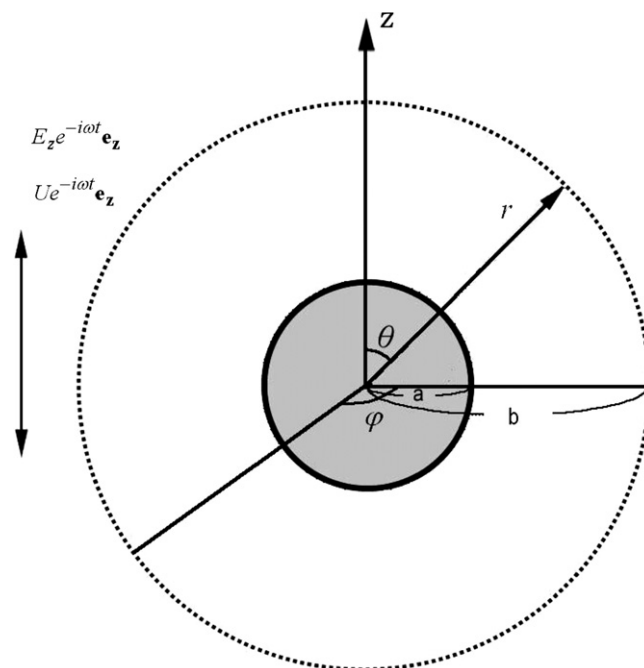


Fig. 1. Geometric configuration of the system in this study.

parts to represent its oscillating nature. The dispersion medium contains $z_1:z_2$ electrolyte, z_1 and z_2 being, respectively, the valences of cations and anions. Kuwabara's (1959) unit cell model is adopted, where a representative droplet is surrounded by a concentric liquid shell of radius b . The spherical coordinates (r, θ, φ) are used with its origin located at the center of the droplet. The physical properties of the electrolyte solution and those of the drop fluid are assumed to maintain constant, and the shape of the drop remains spherical, which will be elaborated later again in this section. Moreover, creeping flow is assumed for the system under consideration.

The electrical potential of the system under consideration, ϕ , can be described by the Poisson equation:

$$\nabla^2 \phi = -\frac{\rho_e}{\varepsilon} = -\sum_{j=1}^2 \frac{z_j e n_j}{\varepsilon}, \quad (1)$$

where ∇^2 is the Laplace operator, ϕ the electrical potential, ρ_e the space charge density, ε the dielectric constant of dispersion medium, e the elementary charge, and n_j the number concentration of ionic species j . The conservation of ionic species j yields

$$\frac{\partial n_j}{\partial t} = \nabla \cdot \left[D_j \left(\nabla n_j + \frac{n_j \hat{e} z_j}{kT} \nabla \phi \right) + n_j \mathbf{u} \right], \quad (2)$$

where ∇ is the gradient operator, D_j the diffusivity of ionic species j , k the Boltzmann constant, and \mathbf{u} the velocity of dispersion medium. Since the Reynolds number is very small, the flow field is described by

$$\nabla \cdot \mathbf{u} = 0, \quad (3)$$

$$\rho \frac{\partial \mathbf{u}}{\partial t} = -\nabla p + \eta \nabla^2 \mathbf{u} - \rho_e \nabla \phi, \quad (4)$$

where p is the pressure, and η and ρ , respectively, the viscosity and the density of the fluid.

Following the same treatment as before (Lee et al., 1999), the variables ϕ , n_j , \mathbf{u} , and p can be decomposed into an equilibrium state plus a perturbed state arising from the applied electric field. The strength of the applied electric field is assumed very weak in comparison with the equilibrium state value established by the charge on the droplet surface. Therefore,

$$\phi(r, \theta, t) = \phi_e(r) + \delta \phi(r, \theta) E_Z e^{-i\omega t}, \quad (5)$$

$$n_j(r, \theta, t) = n_j^e(r, \theta) + \delta n_j(r, \theta) E_Z e^{-i\omega t}, \quad (6)$$

$$\mathbf{u}(r, \theta, t) = \mathbf{0} + \delta \mathbf{u}(r, \theta) E_Z e^{-i\omega t}, \quad (7)$$

$$p(r, \theta, t) = p_e(r, \theta) + \delta p(r, \theta) E_Z e^{-i\omega t}, \quad (8)$$

where the subscript e denotes equilibrium property and the symbol δ represents a perturbed quantity arising from the applied electric field. Note that, for the equilibrium case, since the droplet remains stagnant when the applied electric field is absent, the velocity vanishes. The governing equations and its associated boundary conditions are grouped into two sub-problems: the equilibrium system and the perturbed system as follows.

2.1. Equilibrium system

Since the distribution of ionic species at equilibrium follows Boltzmann distribution, the governing equation for ϕ_e is

$$\nabla^2 \phi_e = -\sum_{j=1}^N \frac{z_j \hat{e} n_{j0}^e}{\varepsilon} \exp\left(-\frac{z_j \hat{e} \phi_e}{kT}\right), \quad a < r < b, \quad (9)$$

$$\nabla^2 \phi_e = 0, \quad 0 < r < a. \quad (10)$$

Eq. (9) is the well-known Poisson–Boltzmann equation. $0 < r < a$ denotes the region inside the drop, and $a < r < b$ represents the dispersion medium. n_{j0}^e is the bulk concentration of ionic species j . Suppose that the potential on the droplet surface is kept constant, and no net electric current across the outer virtual surface, a logic claim reflecting the fact that the bulk system is electrically neutral as a whole. Then the boundary conditions associated with Eqs. (9) and (10) are

$$\phi_e = \zeta_a \quad \text{at } r = a, \quad (11)$$

$$\frac{d\phi_e}{dr} = 0 \quad \text{at } r = b. \quad (12)$$

Moreover,

$$\frac{\partial \phi_e}{\partial r} = 0 \quad \text{at } r = 0 \quad (13)$$

considering the spherical symmetry of the system under consideration.

2.2. Perturbed system

A modified Boltzmann distribution is presented here to account for the polarization effect of the double layer as the droplet is set to motion:

$$n_j = n_{j0}^e \exp\left(-\frac{z_j \hat{e}}{kT} (\phi_e + \delta \phi E_Z e^{-i\omega t} + g_j E_Z e^{-i\omega t})\right), \quad (14)$$

where g_j represents the equivalent perturbed potential arising from double layer polarization (Lee et al., 1999). Substituting Eqs. (5)–(8) and (14) into Eqs. (1)–(4), after some mathematical treatments available elsewhere (Lee et al., 2006), we end up with the governing equations for the perturbed system, which are further divided as

(A) Inside the droplet:

$$-i\omega \rho_i \delta \mathbf{u} E_Z e^{-i\omega t} = -\nabla \delta p E_Z e^{-i\omega t} + \eta_i \nabla^2 \delta \mathbf{u} E_Z e^{-i\omega t}, \quad 0 < r < a, \quad (15)$$

where Eq. (15) is the Navier–Stokes equation in complex form. Note that $\delta \mathbf{u}$ is the perturbed velocity and is a complex quantity with both real and imaginary parts to represent its oscillating nature. Moreover, since Eq. (15) is of complex nature involving complex quantities, there are actually two corresponding equations associated with it, representing real and imaginary parts separately. The associated boundary conditions are

$$\delta u_r E_Z e^{-i\omega t} = 0, \quad r = 0, \quad (16)$$

$$\delta u_\theta E_Z e^{-i\omega t} = 0, \quad r = 0, \quad (17)$$

which are obtained from the symmetric nature of the present problem. Note that there is no electrolyte inside the drop; thus, n_j is zero when $0 < r < a$.

(B) *Outside the droplet:*

The governing equations for the perturbed electric field $\delta\phi$, perturbed ionic concentration δn_j , perturbed pressure δp , and perturbed velocity field $\delta\mathbf{u}$ are, respectively,

$$\begin{aligned} &\nabla^2(\delta\phi E_Z e^{-i\omega t}) \\ &= \sum_{j=1}^2 \frac{z_j \hat{e} n_{j0}^e}{\varepsilon} \left(\exp\left(-\frac{z_j \hat{e}}{kT}(\phi_e + \delta\phi E_Z e^{-i\omega t})\right) \right. \\ &\quad \left. + g_j E_Z e^{-i\omega t} \right) \\ &\quad - \exp\left(-\frac{z_j \hat{e}}{kT} \phi_e\right), \quad a < r < b, \end{aligned} \quad (18)$$

$$\begin{aligned} -i\omega \delta n_j = &-D_j(\nabla^2(\delta n_j) + \frac{z_j \hat{e}}{kT}(\nabla n_j^e \cdot \nabla(\delta n_j) \\ &+ \nabla(\delta n_j) \cdot \nabla \phi_e \\ &+ \nabla(\delta n_j) \cdot \nabla(\delta\phi E_Z e^{-i\omega t}) + n_j^e \nabla^2(\delta\phi) \\ &+ (\delta n_j) \nabla^2 \phi_e \\ &+ (\delta n_j) \nabla^2(\delta\phi E_Z e^{-i\omega t})) \\ &+ (\delta\mathbf{u}) \nabla(n_j^e + \delta n_j E_Z e^{-i\omega t}), \quad a < r < b, \end{aligned} \quad (19)$$

$$\nabla \cdot (\delta\mathbf{u} E_Z e^{-i\omega t}) = 0, \quad a < r < b, \quad (20)$$

and

$$\begin{aligned} -i\omega \rho_o \delta\mathbf{u} E_Z e^{-i\omega t} = &-\nabla \delta p E_Z e^{-i\omega t} + \eta_o \nabla^2 \delta\mathbf{u} E_Z e^{-i\omega t} \\ &- \rho_e \nabla \phi, \quad a < r < b, \end{aligned} \quad (21)$$

where η_i and η_o are, respectively, the viscosity of droplet fluid and that of dispersion medium, and ρ_i and ρ_o are the density of droplet fluid and that of dispersion medium. The associated boundary conditions are

$$\nabla(\delta\phi E_Z e^{-i\omega t}) \cdot \hat{\mathbf{n}} = 0 \quad \text{at } r = a. \quad (22)$$

Eq. (22) indicates that the droplet is non-conducting. At the outer cell surface, Shilov–Zharkikh boundary condition is adopted in the present study, which is derived from thermodynamics consideration relating macroscopic and microscopic electric fields appropriately (Shilov et al., 1981). This model has been successfully applied in concentrated suspensions and yields better agreement with experimental results than the traditional Levine and Neal boundary conditions (Dukhin et al., 1999). Based on the Shilov–Zharkikh boundary condition, we have, after simple arithmetic cancellations,

$$(\delta\phi) = b \cos \theta \quad \text{at } r = b. \quad (23)$$

Since the bulk liquid cannot penetrate a droplet and both the velocity and the shear stress are continuous across the droplet surface, the following conditions are assumed:

$$\delta u_r E_Z e^{-i\omega t} |_{r=a^+} = \delta u_r E_Z e^{-i\omega t} |_{r=a^-} = 0 \quad \text{at } r = a, \quad (24)$$

$$\delta u_\theta E_Z e^{-i\omega t} |_{r=a^+} = \delta u_\theta E_Z e^{-i\omega t} |_{r=a^-} \quad \text{at } r = a, \quad (25)$$

$$(\underline{\underline{\tau}}^n \cdot \mathbf{r}) \times \mathbf{r} |_{r=a^+} = (\underline{\underline{\tau}}^n \cdot \mathbf{r}) \times \mathbf{r} |_{r=a^-} \quad \text{at } r = a, \quad (26)$$

where $\underline{\underline{\tau}}^n$ is the shear stress tensor on the droplet surface. Here, we assume that the cell surface moves with a velocity $-U E_Z e^{-i\omega t}$ relative to a droplet. Also, according to Kuwabara (1959), the vorticity should vanish on the cell surface. Based on these assumptions, the following conditions are assumed on the cell surface:

$$\nabla \times \delta\mathbf{u} E_Z e^{-i\omega t} = 0, \quad r = b \quad (27)$$

$$\delta u_r E_Z e^{-i\omega t} = -(U_R + iU_I) E_Z e^{-i\omega t} \cos \theta, \quad r = b. \quad (28)$$

Here, U_R and U_I are the real and the imaginary parts of the drop velocity.

Moreover, we assume that the surface of the droplet is impermeable to ions; hence, the associated boundary condition of n_j is

$$\frac{\partial n_j}{\partial r} = 0 \quad \text{at } r = a. \quad (29)$$

Besides, no disturbance of concentration of ionic species is allowed at the outer virtual surface; thus, the corresponding boundary conditions for the polarization effect are

$$g_j + \delta\phi = 0 \quad \text{at } r = b. \quad (30)$$

The governing equations, Eqs. (9), (10), (15), (18)–(21), and its associated boundary conditions are then solved by a pseudo-spectral method based on Chebyshev polynomials, which is found to be a powerful and accurate algorithm for the problems of the present type. Note that we have assumed that the droplet remains spherical under the applied oscillating electric field. This is justified as the Weber numbers, both inertial and electrostatic as defined below, of the system are much less than unity (Taylor and Acrivos, 1964; Eow et al., 2003):

$$We = \rho U^2 a / \sigma, \quad (31)$$

$$We_e = \frac{2\varepsilon E^2 a}{\sigma}, \quad (32)$$

where σ is the surface tension of the droplet interface and other variables are defined in the Notations. The dimensionless Weber numbers, We and We_e , are, respectively, measurements of relative significance of inertia force and electric force in comparison with the surface tension, which is the shape-keeping force for the droplet to remain spherical. In the cases under our investigation, which are typical in dynamic electrophoresis, both We and We_e are of the order around 10^{-10} , definitely small enough to justify the spherical-shape assumption for the droplet. Moreover, it also indicates the trivialness of Maxwell stress tensor over the shape of the droplet as far as the deformation of liquid droplet is concerned. However, it would always be a good idea to check the validity of trivial electrostatic Weber number whenever facing an electrophoretic system of liquid droplets.

2.3. Dynamic electrophoretic mobility

The definition of the dynamic electrophoretic mobility μ_m is

$$\mu_m = \mu_R + i\mu_I = \frac{\mathbf{U}}{\mathbf{E}}, \quad (33)$$

where $\mathbf{E} = E_Z e^{-i\omega t}$ and $\mathbf{U} = (U_R + iU_I)E_Z e^{-i\omega t}$, μ_R and μ_I being, respectively, the real and the imaginary parts of μ_m . To obtain μ_m , a force balance exerted on the drop is required. The expression of the force balance is shown as

$$\mathbf{F}_h + \mathbf{F}_e = \frac{4}{3}\pi a^3(\rho_i - \rho_o)\frac{d\mathbf{U}}{dt}, \quad (34)$$

where \mathbf{F}_h and \mathbf{F}_e are, respectively, the hydrodynamic force and the electric force acting on the drop. \mathbf{F}_e and \mathbf{F}_h can be calculated as follows (Happel and Brenner, 1983):

$$\begin{aligned} \mathbf{F}_e &= \iint_S \sigma_e (-\nabla\phi)_s \cdot \mathbf{e}_z dS \\ &= 2\pi\epsilon\epsilon_a^2 \int_0^\pi \left(\frac{\partial\phi}{\partial r}\right)_{r=a} \left(\frac{\partial\phi}{\partial r} \cos\theta - \frac{1}{r} \frac{\partial\phi}{\partial\theta} \sin\theta\right)_{r=a} r^2 \sin\theta d\theta, \end{aligned} \quad (35)$$

$$\begin{aligned} \mathbf{F}_h &= -\pi\rho_o \int_0^\pi \left[r^2 \sin^2\theta \frac{\partial}{\partial t}(\delta\mathbf{u}E_Z e^{-i\omega t})\right]_{r=a} d\theta \\ &+ \eta\pi \int_0^\pi [r^2 \sin^2\theta (\nabla^2 \delta\mathbf{u}E_Z e^{-i\omega t})]_{r=a} d\theta \\ &- \pi \int_0^\pi [r^2 \sin^2\theta \rho_e (\nabla\phi)]_{r=a} d\theta, \end{aligned} \quad (36)$$

where S denotes the droplet surface and σ_e the surface charge density, determined by Gauss law. For an easier treatment, we iterate the velocity of the droplet under some applied electric field $E_Z e^{-i\omega t}$ until Eq. (34) is satisfied. Since the dynamic electrophoretic mobility is a complex number, it can be characterized by its magnitude $\mu_m = \sqrt{\mu_R^2 + \mu_I^2}$ and phase angle $\Theta = \tan^{-1}(\mu_I/\mu_R)$. Thus, $\mathbf{E} = E_Z e^{-i\omega t} \mathbf{e}_z$ and $\mathbf{U} = \sqrt{U_R^2 + U_I^2} E_Z e^{-i\omega t + \Theta} \mathbf{e}_z$, $\Theta < 0$ implies that \mathbf{U} leads \mathbf{E} , and the reverse is true if $\Theta > 0$.

3. Results and discussion

Since a variety of important factors might influence the electrophoretic behavior of the system under consideration, we group them in dimensionless form to simplify the analysis. They include: the scaled dynamic electrophoretic mobility $\mu_m^* = \mu/(\epsilon\epsilon_a/\eta)$, the scaled frequency $\omega^* = \rho_o \omega a^2/\eta_o$, the scaled double layer thickness κa , where $\kappa^{-1} = (\epsilon kT/\sum_{j=1}^2 n_{j0}^e (ez_j)^2)^{1/2}$, the viscosity ratio (η_o/η_i), the scaled surface potential $\phi_r = z_1 e\zeta_a/kT$, and the volume fraction of droplets, measured by $H = (a/b)^3$. The following values are also assumed in numerical simulations: $T = 298.15$ K, $z_1 = -z_2 = 1$, $\eta_o = 8.904 \times 10^{-3}$ g/cm s, $\rho_o/\rho_i = 0.909$, and $\epsilon = 8.854 \times 10^{-12} \times 78.54688$ F/m, typical for aqueous KCl solution.

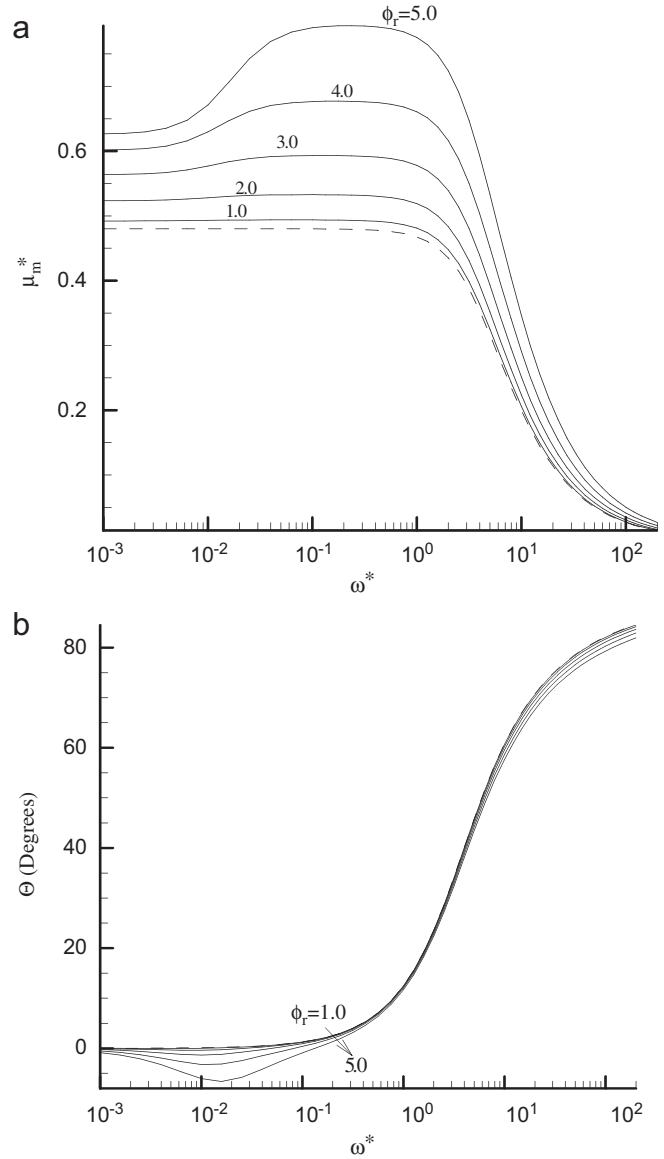


Fig. 2. Variation in the scaled magnitude of dynamic electrophoretic mobility μ_m^* (a), and phase angle Θ (b), as a function of the scaled frequency ω^* for various values of ϕ_r at $\kappa a = 1$, $H = 0.1$, and $\eta_o/\eta_i = 1$. Dash line: low zeta potential.

3.1. Effect of frequency and surface potential

Figs. 2–5 show the variations in the scaled magnitude of electrophoretic mobility μ_m^* , and the corresponding phase angle Θ , as functions of the scaled frequency of the applied electric field ω^* at various values of ϕ_r . For the purpose of comparison, corresponding results of low zeta potential presented by Hsu et al. (2007) are also shown in the graphs. Clearly our results approach the limiting case as $\phi_r \rightarrow 0$. Actually as $\phi_r = 1$, they still almost coincide with each other in lots of cases shown. With even higher ϕ_r , however, the outcome is quite different. For low surface potential, the mobility μ_m^* monotonically decreases with increasing frequency. Examining Eqs. (15) and (21) closely, as ω^* gets larger, the flow field will be dominated

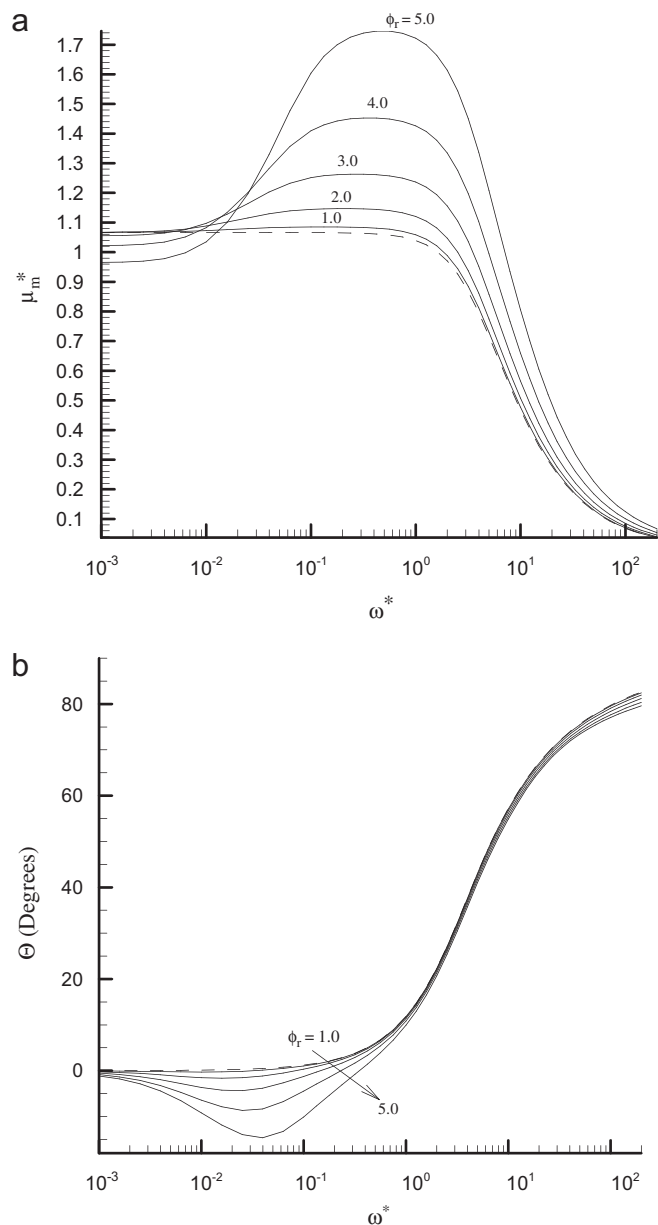


Fig. 3. Variation in the scaled magnitude of dynamic electrophoretic mobility μ_m^* (a), and phase angle Θ (b), as a function of the scaled frequency ω^* for various values of ϕ_r at $\kappa a = 3$, $H = 0.1$, and $\eta_o/\eta_i = 1$. Dash line: low zeta potential.

by the inertia term, and the influences of the other terms diminish. Moreover, as the direction of the applied electric field changes back and forth, the direction of the drop motion will change accordingly. And eventually the drop simply fails to keep up with the rapid pace of the applied AC field as ω^* gets large, as we reported and explained in a related paper earlier (Hsu et al., 2007). However, the mobilities corresponding to high surface potentials here increase first, and then decrease rapidly with increasing ω^* , exhibiting maximums at medium to high frequencies. In the case of static electric field, double layer polarization induces an internal electric field in the opposite direction of the externally applied one, hence retarding

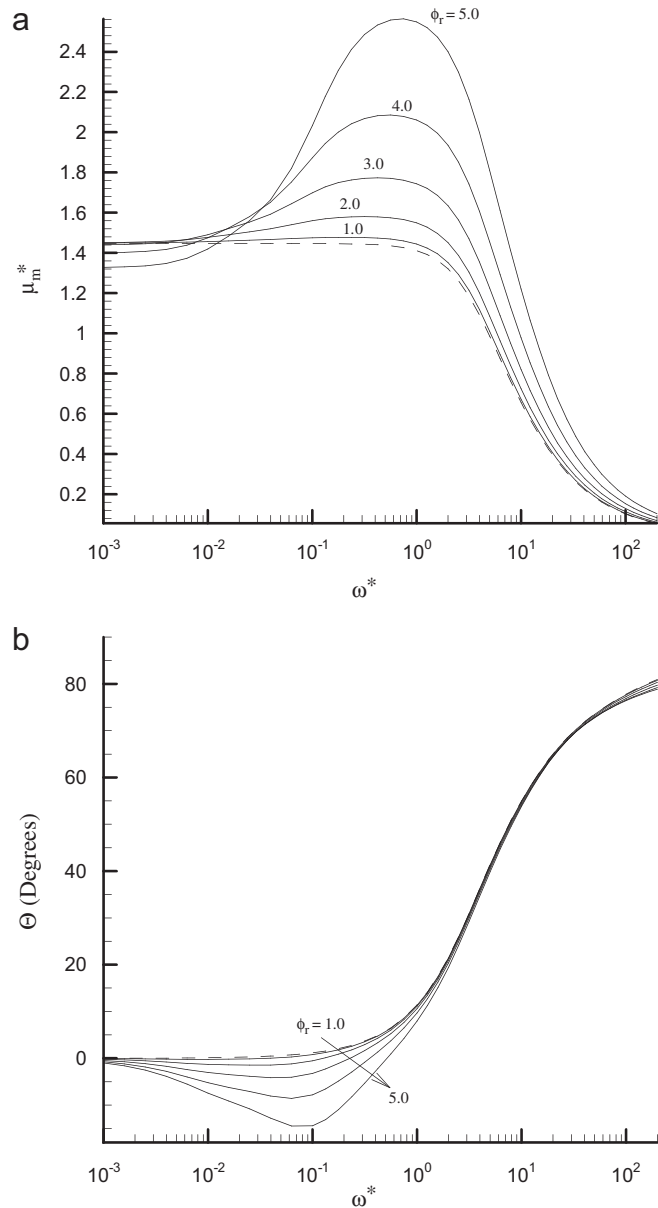


Fig. 4. Variation in the scaled magnitude of dynamic electrophoretic mobility μ_m^* (a), and phase angle Θ (b), as a function of the scaled frequency ω^* for various values of ϕ_r at $\kappa a = 5$, $H = 0.1$, and $\eta_o/\eta_i = 1$. Dash line: low zeta potential.

the movement of drops. Generally speaking, with the increase in ϕ_r , the polarization effect becomes even more significant. However, if a dynamic electric field is applied, its direction changes with time and the corresponding induced electric field cannot respond instantly. A phase lag is generally observed as a result. It is interesting to note that the associated phase angle Θ observed here becomes even negative at medium ω^* , indicating the response of the drop velocity leads that of the applied electric field. This is certainly impossible from the viewpoint of cause and consequence: How can a response take place before the input signal is yet introduced? The apparent phase lead by the dynamic electrophoresis signal over the input AC field

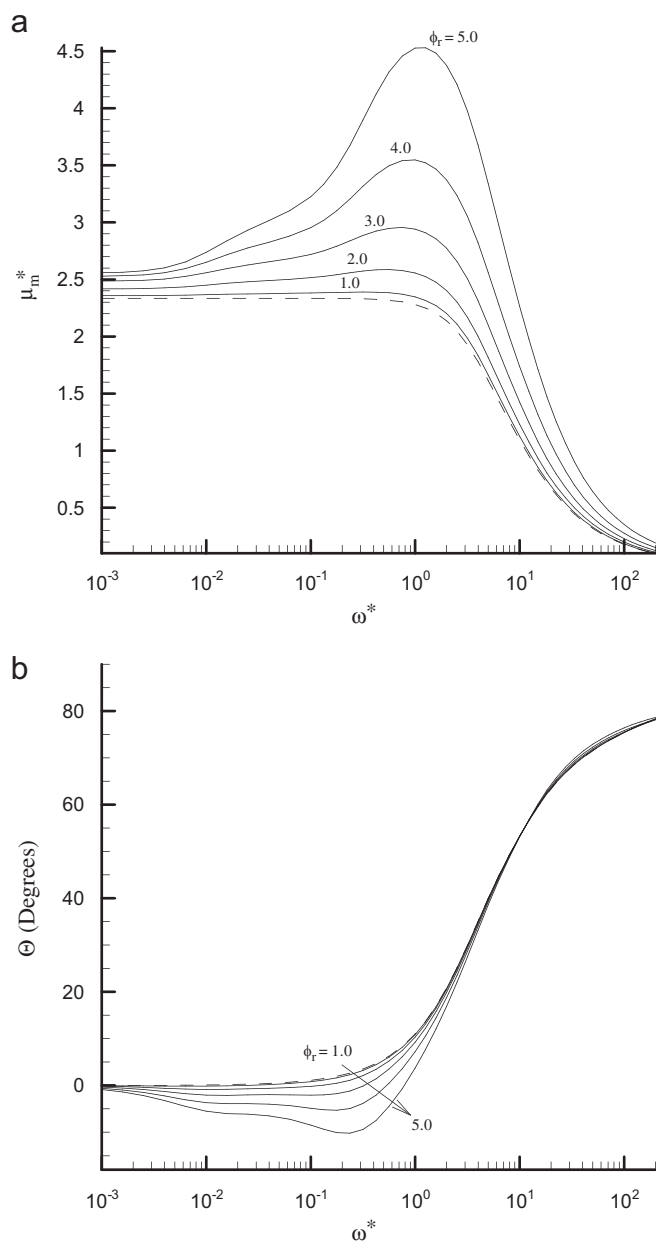


Fig. 5. Variation in the scaled magnitude of dynamic electrophoretic mobility μ_m^* (a), and phase angle Θ (b), as a function of the scaled frequency ω^* for various values of ϕ_r at $\kappa a = 10$, $H = 0.1$, and $\eta_o/\eta_i = 1$. Dash line: low zeta potential.

is simply an indication of a way too slow response that actually lag an entire period. Thus, the induced electric field due to polarization may actually accelerate the movement of the drops and result in an ascending trend of the mobility curves. And similar to the situation at low zeta potential, as ω^* further increases, eventually the accelerating time in each individual period becomes so short, due to the fast offset by the back and forth rapid changing of input AC field, that the mobility actually goes down again, and the polarization effect, hence, is not important anymore. The combined effects mentioned above generate the maxima as observed in Figs. 2(a)–5(a). The peaks

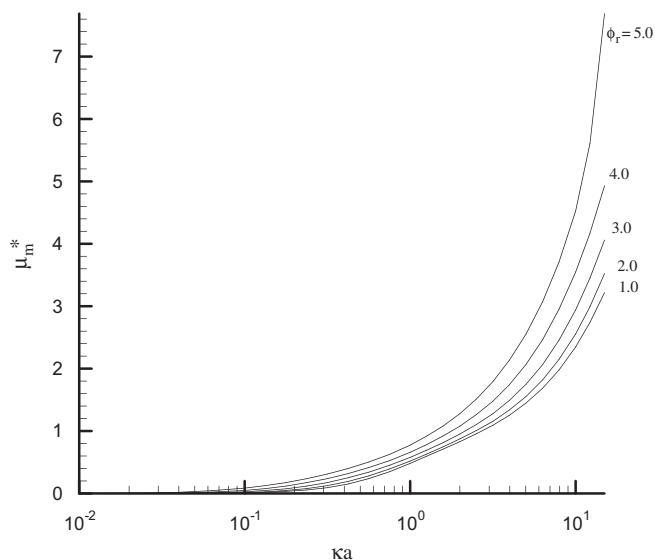


Fig. 6. Variation in the scaled magnitude of electrophoretic mobility μ_m^* as a function of κa for various values of ϕ_r at $\omega^* = 1$, $\eta_o/\eta_i = 1$, and $H = 0.1$.

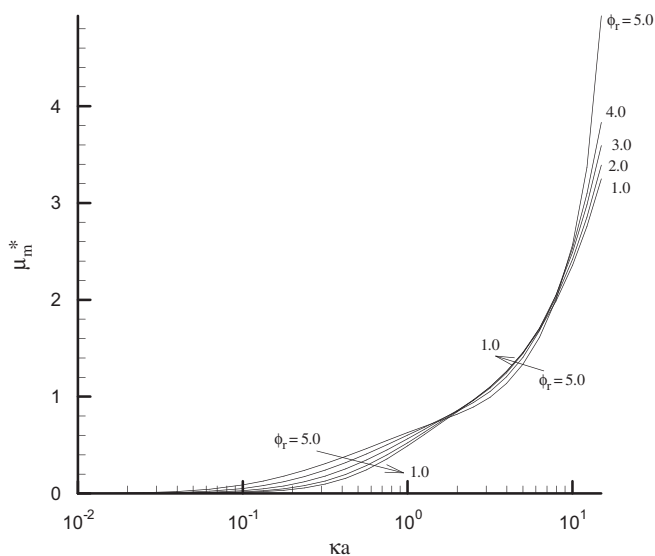


Fig. 7. Variation in the scaled magnitude of electrophoretic mobility μ_m^* for various values of ϕ_r at $\omega^* = 0.002$, $\eta_o/\eta_i = 1$, and $H = 0.1$.

shown in Figs. 2(a)–5(a) also become more pronounced as ϕ_r increases. Also, as ω^* gets large, the time for drops to react by altering its direction of movement becomes short; hence, the phase lag increases accordingly. Figs. 2(b)–5(b) reveal this phenomenon in the present problem.

3.2. Effect of double layer thickness

The effect of double layer thickness on the dynamic electrophoretic mobility is different for high or low frequency, as shown in Figs. 6 and 7. In Fig. 6, $\omega^* = 1$, which corresponds to a dimensional frequency of about 10 MHz ($a = 300$ nm) here, and is considered a high frequency situation in typical

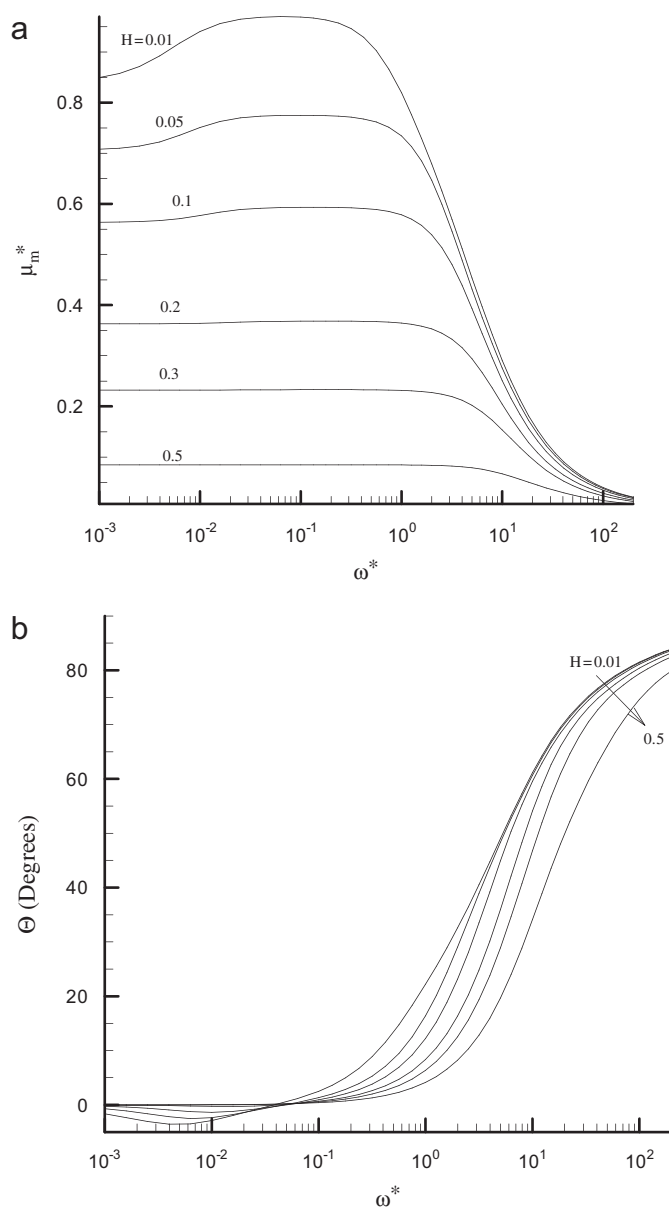


Fig. 8. Variation in the scaled magnitude of dynamic electrophoretic mobility μ_m^* (a), and phase angle Θ (b), as a function of the scaled frequency ω^* for various values of H at $\kappa a = 1$, $\phi_r = 3$, and $\eta_o/\eta_i = 1$.

dynamic electrophoresis. The dynamic electrophoretic mobility increases monotonically with κa in the range of 1–10. This is because the polarization effect, i.e., the distortion of ionic cloud within the double layer, is dampened due to phase lag, as explained in the last paragraph, thus no longer a significant factor. The mobility is mainly determined by such factors as surface potential and double layer thickness. As κa increases, indicating the double layer gets thinner, thus less “hindrance effect” from double layer overlapping with neighboring droplets, the mobility hence increases monotonically as shown in Fig. 6. In Fig. 7, $\omega^* = 0.002$, which corresponds to a dimensional frequency of about 20 kHz, a low frequency in typical dynamic electrophoresis. The situation here is kind of complicated, and we see a reverse of ϕ_r dependence of μ_m^* as κa

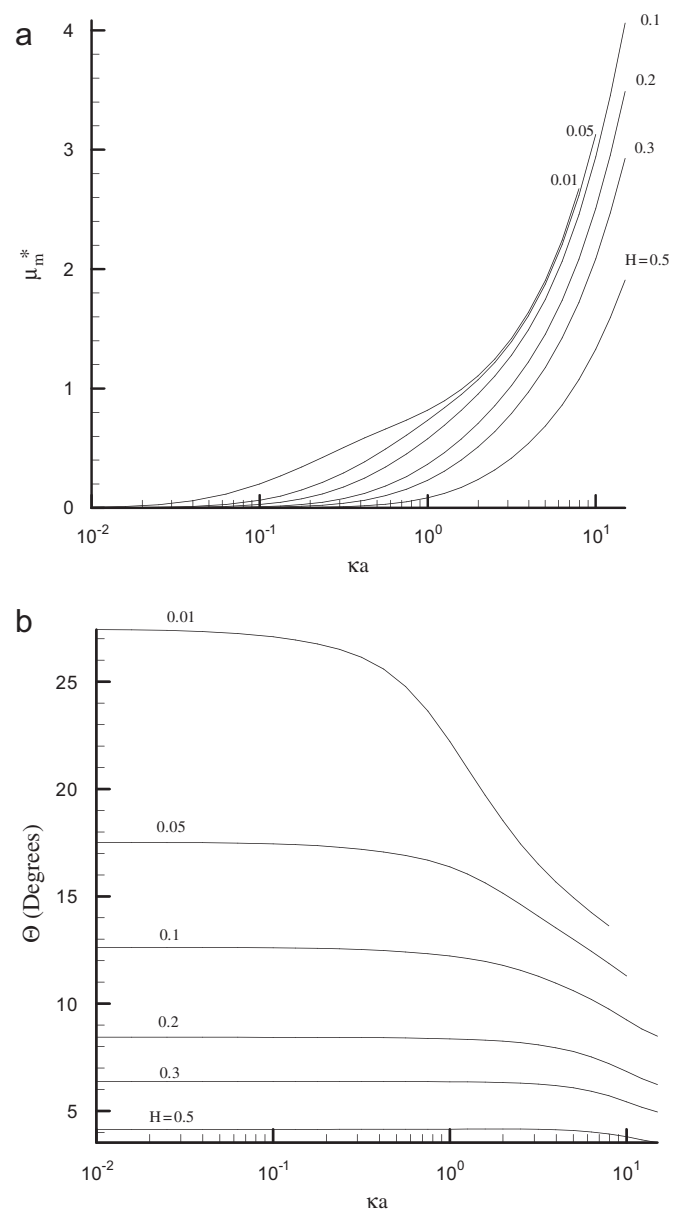


Fig. 9. Variation in the scaled magnitude of electrophoretic mobility μ_m^* (a), and phase angle Θ (b), as a function of κa for various values of H at $\omega^* = 1$, $\eta_o/\eta_i = 1$, and $\phi_r = 3$.

increases, which is absent in the previous high frequency case ($\omega^* = 1$). Again, polarization effect is the determining factor behind it. Taking a closer look at Fig. 7, we found that if the double layer becomes thinner (κa increases) but still comparable with the droplet radius, the additional electrohydrodynamic interactions due to double layer overlapping from neighboring drops decrease, and the distortion of ionic cloud near the charged surface becomes more significant. As a result, the induced electric force mentioned on the last paragraph will have a significant retarding effect on the movement of drops. As κa increases further, however, the double layer thickness gets so thin that eventually the distortion of the ionic cloud becomes negligible again, and the dynamic electrophoretic mobility restores to its previous behavior, i.e., to increase accordingly with

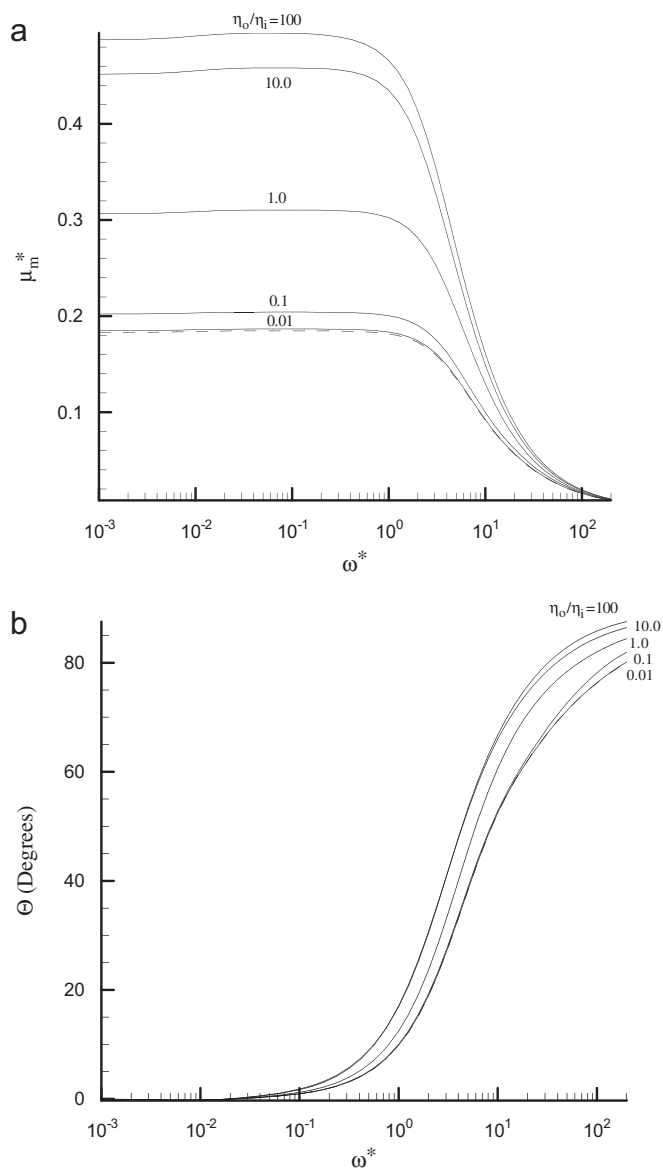


Fig. 10. Variation in the scaled magnitude of electrophoretic mobility μ_m^* (a), and phase angle Θ (b), as a function of ω^* for various values of η_o/η_i at $H = 0.1$, $\kappa_a = 0.5$, and $\phi_r = 3$. Dash line: hard spherical particle.

increasing surface potential. Similar behaviors are also observed in the case of an isolated spherical particle (Preston et al., 2005) and concentrated dispersion of spherical particles (Hsu et al., 2002), both at high surface potential.

3.3. Effect of volume fraction

The effect of volume fraction H is presented in Figs. 8 and 9. It is obvious that μ_m^* and Θ decrease with the increase in volume fraction H . This is because as the volume fraction of drops gets large, the distance between droplets becomes narrow. For example, if the volume fraction of drops changes from $H = 0.1$ to 0.2 , the dimensionless distance between droplets, $2(b - a)$, would be shortened approximately from 2.3 to 1.42. Double layer overlapping may occur in the current analysis if

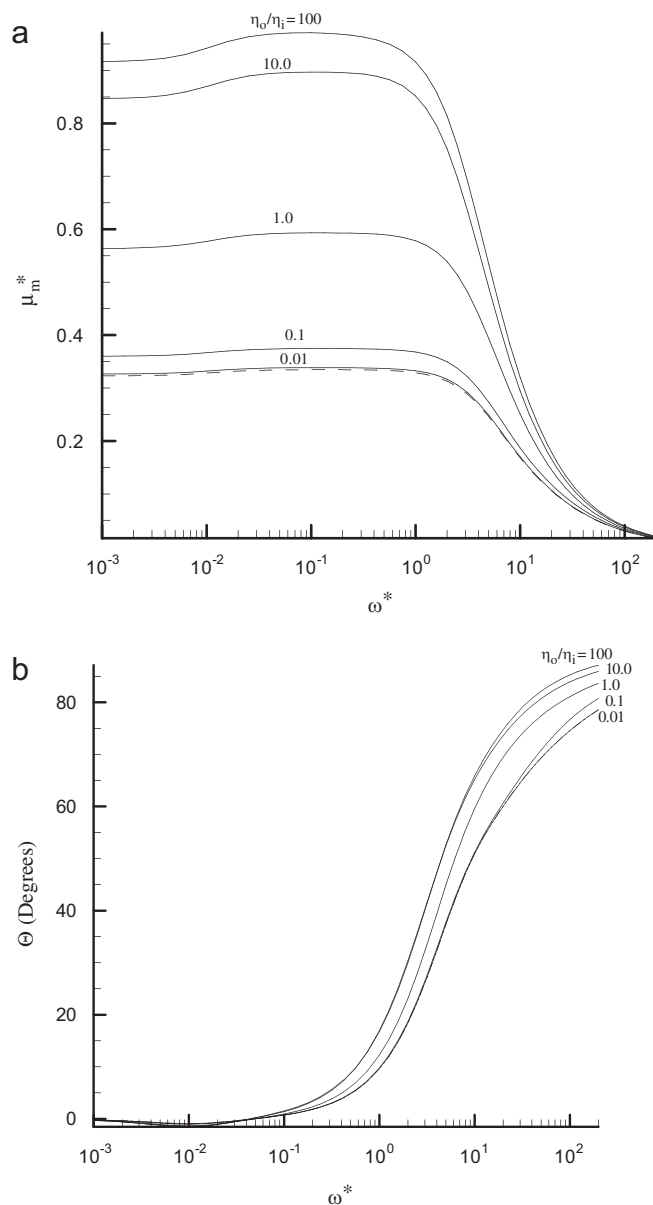


Fig. 11. Variation in the scaled magnitude of electrophoretic mobility μ_m^* (a), and phase angle Θ (b), as a function of ω^* for various values of η_o/η_i at $H = 0.1$, $\kappa_a = 1.0$, and $\phi_r = 3$. Dash line: hard spherical particle.

the electrolyte concentration is low (small κa) or the drops become concentrated (large H). The influence of the double layer thickness surrounding a drop on its electrophoretic behavior is also illustrated in Fig. 9. In the limit as $\kappa a \rightarrow 0$, the magnitude of the dynamic mobility always decreases to zero, as expected. This is because as $\kappa a \rightarrow 0$, the thickness of the double layer surrounding the drop surface gets infinitely thick, hence influencing all the other drops throughout the entire dispersion system. Due to the double layer overlapping effect, it actually yields a uniform distribution of ions and thus a uniform electric potential in the solution. As a result, no electric force is generated upon the drop and it remains stationary. However, the effect of double layer overlapping gradually disappears with the increase in κa or the decrease in volume fraction, yielding

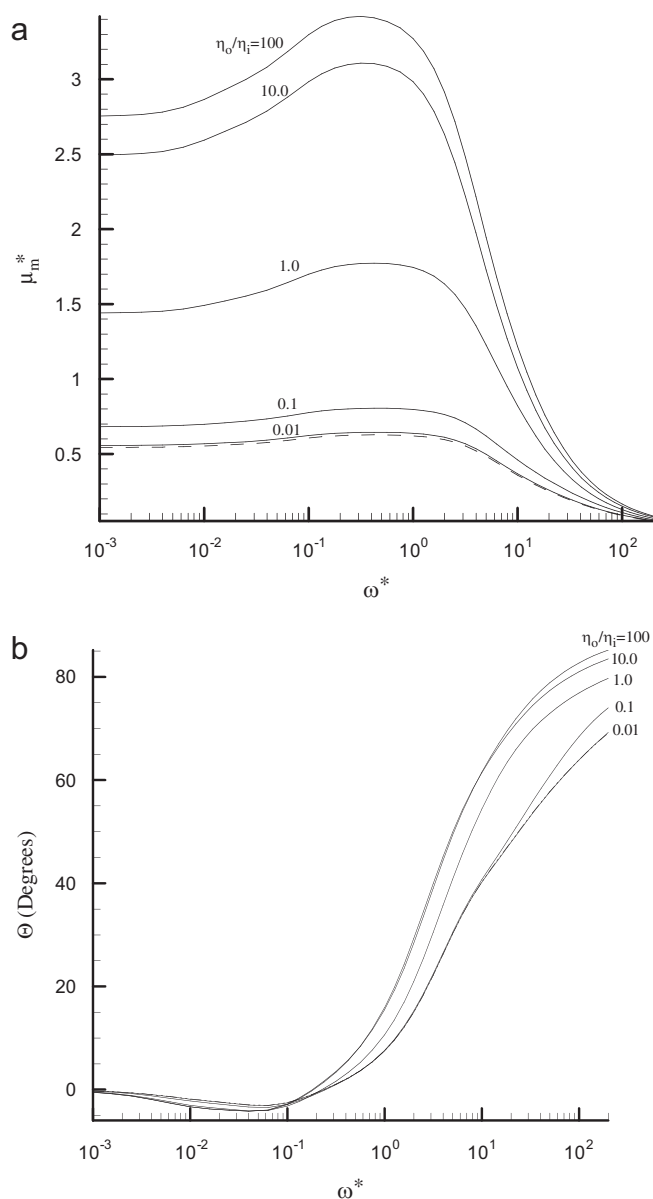


Fig. 12. Variation in the scaled magnitude of electrophoretic mobility μ_m^* (a), and phase angle Θ (b), as a function of ω^* for various values of η_o/η_i at $H = 0.1$, $\kappa a = 5.0$, and $\phi_r = 3$. Dash line: hard spherical particle.

a non-uniform distribution of ions, which sets up the motion eventually. The higher the κa , the less significant the double layer overlapping from neighboring drops, and the mobility increases accordingly. The drop is also easier to respond to the variation in the applied electric field with less entanglement from the double layer overlapping. Thus, the phase lag Θ in Fig. 9(b) decreases with increasing κa . This is because the electrical double layer is confined to a narrow space, and the time necessary to adjust the ionic distribution inside is short, and the phase lag is getting smaller.

3.4. Effect of viscosity ratio

Probably the most important factor affecting the dynamic electrophoresis of a droplet is its viscosity. After all, that is what

set it apart from the conventional studies on the rigid sphere. The influence of the viscosity of the droplet fluid at several κa on its electrophoretic behavior is illustrated in Figs. 10–12. These figures reveal that the larger the ratio of (η_o/η_i) , the larger the μ_m^* . This is because as η_i gets small, the fluid inside the droplet is easier to flow; hence, the shear rate at the droplet surface decreases and results in a smaller retarding drag force. The mobility of the droplets thus increases with declining η_i . In comparison, corresponding results of rigid spherical particles (Hsu et al., 2002) are also presented in Figs. 10–12. As can be clearly seen from these figures, they serve as the limiting cases as (η_o/η_i) approaches zero. The phase lag is also found to increase with larger (η_o/η_i) , since longer time is needed for the “lighter” (less viscous) internal fluid to react accordingly. The influence of (η_o/η_i) on the phase lag is not as substantial as that on the mobility magnitude μ_m^* , though. Figs. 10–12 serve as an extension of the traditional dynamic electrophoresis data for dispersions of rigid colloids.

4. Conclusion

The dynamic electrophoretic behavior of a concentrated dispersion of drops with arbitrary surface potential is investigated. The effect of volume fraction of drops and double layer thickness is examined in particular. In summary, we conclude the following:

- (i) If the zeta potential on droplet surface is high, the effect of double layer polarization cannot be neglected. The dynamic electrophoretic mobility exhibits a maximum as a result and then decreases rapidly with increasing frequency of AC field.
- (ii) At medium frequency, the induced electric force coming from the distortion of ionic cloud may actually accelerate the movement of drops. However, with further increase in the frequency, the time for drops to alter its direction of movement becomes short, which slows down the mobility. The phase lag increases accordingly.
- (iii) The magnitude of electrophoretic mobility declines with the volume fraction of droplets due to the hindrance effect and electrostatic interaction from neighboring drops.
- (iv) The effect of double layer overlapping is very significant in concentrated dispersion if the volume fraction of drops is high and the double layer is thick.
- (v) The smaller the viscosity of the droplet fluid, the larger the magnitude of dynamic electrophoretic mobility and the phase lag. As the viscosity of the droplet fluid increases, the electrophoretic behavior of a droplet approaches that of a rigid particle eventually.

Notation

| | |
|-------|--------------------------------------------------|
| a | radius of droplets, m |
| b | radius of the liquid shell, m |
| D_j | the diffusivity of ionic species j , m^2/s |
| e | charge of electron (1.6×10^{-19} Coul) |
| e_z | z -component of Cartesian coordinates |

| | |
|----------|----------------------------------------------------------------|
| E | applied AC electric field, V/m |
| E_z | strength of the AC electric field, V/m |
| F_e | electrical force, N |
| F_h | hydrodynamic force, N |
| g_j | the potential function for the double layer polarization, V |
| H | volume fraction of droplets, dimensionless |
| I | $i = \sqrt{-1}$ |
| k | Boltzmann constant (1.38×10^{-23} J/K) |
| n_j | number density of electrolytes j , number/m ³ |
| n_{j0} | bulk concentration of electrolytes j , number/m ³ |
| p | pressure, N/m ² |
| r | r -component of spherical coordinates |
| T | absolute temperature, K |
| t | time, s |
| u | velocity of dispersion medium, m/s |
| U | terminal velocity of the droplets, m/s |
| We | inertia Weber number, dimensionless |
| We_e | electrostatic Weber number, dimensionless |
| z_i | valence of ionic species i , dimensionless |

Greek letters

| | |
|----------------------|-------------------------------------------------------------|
| ε | dielectric constant of dispersion medium, C/V/m |
| ζ_a | surface potential on the droplets, V |
| η | fluid viscosity, kg/m/s |
| η_i | fluid viscosity inside of the droplets, kg/m/s |
| η_o | fluid viscosity outside the droplets, kg/m/s |
| θ | θ -component of spherical coordinates |
| Θ | phase angle between velocity and electric field, deg |
| κ | reciprocal Debye length, m ⁻¹ |
| μ_m | dynamic electrophoretic mobility, m ² /V/s |
| ρ | fluid density, kg/m ³ |
| ρ_e | space charge density in dispersion medium, C/m ³ |
| ρ_i | fluid density inside the droplets, kg/m ³ |
| ρ_o | fluid density outside the droplets, kg/m ³ |
| σ | surface tension, kg/s ² |
| σ_e | surface charge density, C/m ² |
| $\underline{\tau}^n$ | shear stress tensor, kg/m/s ² |
| ϕ | electrical potential, V |
| ϕ_r | scaled surface potential on the droplets, dimensionless |
| φ | φ -component of spherical coordinates |
| ω | dynamic frequency of the AC electric field, s ⁻¹ |

Superscripts

* scaled symbols

Subscript

| | |
|----------|-----------------------------------|
| e | equilibrium properties |
| S | properties on the droplet surface |
| δ | perturbed properties |

References

- Baygents, J.C., Saville, D.A., 1991a. Electrophoresis of drops and bubbles. *Journal of Chemical Society, Faraday Transactions* 87, 1883–1898.
- Baygents, J.C., Saville, D.A., 1991b. Electrophoresis of small particles and fluid globules in weak electrolytes. *Journal of Colloid and Interface Science* 146, 9–37.
- Booth, F., 1951. The cataphoresis of spherical fluid droplets in electrolytes. *Journal of Chemical Physics* 19, 1331–1342.
- Dukhin, A.S., Shilov, V.N., Ohshima, H., Goetz, P.J., 1999. Electroacoustic phenomena in concentrated dispersions: new theory and CVI experiment. *Langmuir* 15, 6692–6706.
- Dukhin, A.S., Goetz, P.J., Wines, T.H., Somasundaran, P., 2000. Acoustic and electroacoustic spectroscopy. *Colloid and Surfaces A: Physicochemical and Engineering Aspects* 173, 127–158.
- Eow, J.S., Ghadiri, M., Sharif, A., 2003. Experimental studies of deformation and break-up of aqueous drops in high electric fields. *Colloids and Surfaces A: Physicochemical and Engineering Aspects* 225, 193–210.
- Happel, J., Brenner, H., 1983. *Low-Reynolds Number Hydrodynamics*. Martinus Nijhoff, Dordrecht.
- Hsu, J.P., Lee Eric, Yen, F.Y., 2002. Dynamic electrophoretic mobility in electroacoustic phenomenon: concentrated dispersions at arbitrary potentials. *Journal of Physical Chemistry B* 106, 4789–4798.
- Hsu, J.P., Min, W.L., Lee, E., 2007. Dynamic electrophoresis of droplet dispersions at low surface potentials. *Journal of Colloid and Interface Science* 306, 421–427.
- Hunter, R.J., 1998. Recent developments in the electroacoustic characterization of colloidal suspensions and emulsions. *Colloids and Surfaces A: Physicochemical and Engineering Aspects* 141, 37–65.
- Kuwabara, S., 1959. The forces experienced by randomly distributed parallel circular cylinders or spheres in a viscous flow at small Reynolds numbers. *Journal of the Physical Society of Japan* 14, 527–539.
- Lee, E., Chu, J.W., Hsu, J.P., 1999. Electrophoretic mobility of a concentrated suspension of spherical particles. *Journal of Colloid and Interface Science* 209, 240–246.
- Lee, E., Yen, F.Y., Hsu, J.P., 2001. Dynamic electrophoretic mobility of concentrated spherical dispersions. *Journal of Physical Chemistry B* 105, 7239–7245.
- Lee, E., Fu, C.H., Hsu, J.P., 2002a. Dynamic electrophoretic mobility of a concentrated dispersion of particles with a charge-regulated surface at arbitrary potential. *Journal of Colloid and Interface Science* 250, 327–336.
- Lee, E., Lee, Y.H., Pai, Y.T., Hsu, J.P., 2002b. Flow of a viscoelastic shear-thinning fluid between two concentric rotating spheres. *Chemical Engineering Science* 57, 507–514.
- Lee, E., Tung, C.P., Hsu, J.P., 2003. Dynamic electrophoretic mobility of a sphere in a spherical cavity. *Journal of Colloid and Interface Science* 260, 118–125.
- Lee, E., Ming, J.K., Hsu, J.P., 2004. Purely viscous flow of a shear-thinning fluid between two rotating spheres. *Chemical Engineering Science* 59, 417–424.
- Lee, E., Ming, W.L., Hsu, J.P., 2006. Dynamic electrophoretic mobility of a droplet in a spherical cavity. *Langmuir* 22, 3920–3928.
- Levine, S., O'Brien, R.N., 1973. Theory of electrophoresis of charged mercury drops in aqueous-electrolyte solution. *Journal of Colloid and Interface Science* 43, 616–629.
- Lou, S.H., Lee, E., Hsu, J.P., 2005. Dynamic electrophoresis of a sphere in a spherical cavity: arbitrary surface potential. *Journal of Colloid and Interface Science* 285, 865–871.
- Mangelsdorf, C.S., White, L.R., 1992. Electrophoretic mobility of a spherical colloidal particle in an oscillating electric-field. *Journal of the Chemical Society, Faraday Transactions* 88, 3567–3581.
- Mizuno, D., Kimura, Y., Hayakawa, R., 2000. Dynamic electrophoretic mobility of colloidal particles measured by the newly developed method of quasi-elastic light scattering in a sinusoidal electric field. *Langmuir* 16, 9547–9554.
- O'Brien, R.W., 1988. Electroacoustic effects in a dilute suspension of spherical particles. *Journal of Fluid Mechanics* 190, 71–86.
- O'Brien, R.W., Cannon, D.W., Rowlands, W.N., 1995. Electroacoustic determination of particle size and zeta potential. *Journal of Colloid and Interface Science* 173, 406–418.
- Ohshima, H., 1996. Dynamic electrophoretic mobility of a spherical colloidal particle. *Journal of Colloid and Interface Science* 179, 431–438.
- Ohshima, H., 1997. Dynamic electrophoretic mobility of spherical colloidal particles in concentrated suspensions. *Journal of Colloid and Interface Science* 195, 137–148.

- Ohshima, H., 1999a. Dynamic electrophoretic mobility of spherical colloidal particles with thin electrical double layers in concentrated suspensions. *Colloid and Surfaces A: Physicochemical and Engineering Aspects* 149, 5–11.
- Ohshima, H., 1999b. Dynamic electrophoretic mobility of spherical colloidal particles in concentrated suspensions: approximation of nonoverlapping double layers. *Colloid and Surfaces A: Physicochemical and Engineering Aspects* 159, 293–297.
- Ohshima, H., 1999c. Electrokinetic phenomena in a concentrated dispersion of charged mercury drops. *Journal of Colloid and Interface Science* 218, 535–544.
- Preston, M.A., Kornbrekke, R., White, L.R., 2005. Determination of the dynamic electrophoretic mobility of a spherical colloidal particle through a novel numerical solution of the electrokinetic equations. *Langmuir* 21, 9832–9842.
- Shilov, V.N., Zharkikh, N.I., Borkovskaya, Y.B., 1981. Theory of non-equilibrium electrostatic phenomena in concentrated disperse systems. 1. Application of non-equilibrium thermodynamics to cell model of concentrated dispersions. *Colloid Journal of the USSR* 43, 434–438.
- Taylor, T.D., Acrivos, A., 1964. On the deformation and drag of falling viscous drop at low Reynolds number. *Journal of Fluid Mechanics* 18, 466–476.